



Published in final edited form as:

Rep U.S. 2018 October ; 2018: 2292–2298. doi:10.1109/IROS.2018.8594023.

A Phase Variable Approach to Volitional Control of Powered Knee-Ankle Prostheses

Siavash Rezazadeh, David Quintero, Nikhil Divekar, and Robert D. Gregg

Locomotor Control Systems Laboratory, Departments of Bioengineering and Mechanical Engineering, The University of Texas at Dallas, Richardson, TX 75080, USA

Abstract

Although there has been recent progress in control of multi-joint prosthetic legs for periodic tasks such as walking, volitional control of these systems for non-periodic maneuvers is still an open problem. In this paper, we develop a new controller that is capable of both periodic walking and common volitional leg motions based on a piecewise holonomic phase variable through a finite state machine. The phase variable is constructed by measuring the thigh angle, and the transitions in the finite state machine are formulated through sensing foot contact together with attributes of a nominal reference gait trajectory. The controller was implemented on a powered knee-ankle prosthesis and tested with a transfemoral amputee subject, who successfully performed a wide range of periodic and non-periodic tasks, including low- and high-speed walking, quick start and stop, backward walking, walking over obstacles, and kicking a soccer ball. The proposed approach is expected to provide better understanding of volitional motions and lead to more reliable control of multi-joint prostheses for a wider range of tasks.

I. Introduction

From a biomechanics perspective, the human gait cycle can be divided into different phases (e.g., stance and swing phase) and sub-phases (e.g., weight acceptance, push-off, early swing, etc.), each serving a specific purpose in locomotion [1]. This perspective was preserved in control design for powered lower limb prostheses, which involves first detecting the correct sub-phase and then controlling that particular behavior of the prosthetic joints [2]–[6]. The tuning has to be performed separately for each individual based on various physical parameters, e.g., body mass, as well as functional parameters, e.g., gait pattern. Due to the large number of parameters that need to be manually tuned, the process is typically arduous and difficult to automate, often taking multiple hours for each subject [4].

To address these issues, recent efforts have been based around parameterizing the gait cycle over a phase variable, i.e., a monotonic signal that represents the progression through the cycle. Aside from the ability of parameterizing the gait, ideally the phase variable is invariant across different subjects and does not depend on parameters such as the person's mass or height. In [7], the heel-to-toe movement of the Center of Pressure (CoP) served as the phase variable for determining progression through the stance phase, whereas the swing

phase was controlled by two impedance-based states. In [8], the authors investigated additional phase variables for locomotion and found that the global thigh angle is a suitable piecewise monotonic signal that can be used to control the stance and swing phases separately. By also using the integral of the global thigh angle, a phase variable continuous across the gait cycle was derived and tested with amputee subjects [9].

Everyday tasks comprise both rhythmic activities, such as walking, and non-rhythmic activities, such as stepping over obstacles. A controller strictly based on behavior in a cyclic task, such as the unified controller presented in [9], will encounter problems for non-rhythmic volitional motions. In previous studies such as [10]–[12], volitional control ability was enhanced using electromyography (EMG) signals from the residual limb. However, EMG can be affected by multiple physical, physiological, and anatomical factors making it an unreliable signal source that requires complex signal processing [13]. We therefore seek a more reliable solution using only mechanical measurements.

As a first attempt for such a control scheme, Villarreal et al. used the thigh angle and a stance/swing detection switch to implement a piecewise phase variable for volitional control [14]. However, the controller was problematic during transitions, as using solely the foot contact condition for transition between stance and swing phase variables would result in jumps and oscillations. To avoid such jumps, pushoff was eliminated, but consequently made walking at greater speeds difficult and inefficient. Moreover, the undesired jumps would still occur when standing, as the subject shifted their weight to the sound leg.

In this paper, we present a phase-based control scheme that can manage both natural walking with different speeds and volitional tasks, while avoiding undesirable jumps and oscillations. We first define a piecewise holonomic phase variable based on the thigh angle and utilize it to parameterize the kinematic trajectories obtained from human data. Next, we design a Finite State Machine (FSM) to appropriately change the phase variable definition (and as a result, the parameterization) based on different operating conditions. The proposed FSM only adjusts the kinematic-based phase variable and does not change the controller itself, which remains the same through all conditions/states. We investigate the control method, its benefits, and its limitations through a set of experiments with an amputee subject. Specifically, periodic tasks are tested by walking at different speeds on a treadmill, and non-periodic tasks are tested by experiments such as walking overground with variable speed, backward walking, crossing an obstacle, and kicking a soccer ball.

II. Control Design

This section presents the design of the proposed scheme for volitional and periodic control of a powered knee-ankle prosthesis. First, we explain the use of virtual constraints for formulating the desired knee and ankle joint trajectories. Next, we describe the design of our proposed phase variable for parameterizing the virtual constraints in different stages of the gait cycle. Finally, we discuss how the controller is implemented on a powered prosthesis.

A. Virtual Constraints

Virtual constraints, as introduced in [15], [16], are a useful tool to represent time-invariant trajectories, which can considerably simplify the process of controlling periodic orbits. Originally, virtual constraints were introduced as relationships among generalized positions (angles), which is analogous to a holonomic set of kinematic constraints. More recently, nonholonomic virtual constraints have also been used in legged robots applications [17], [18]. Generally, virtual constraints define the desired trajectories for the controlled degrees of freedom in the following form:

$$q_i^d = h(s), \quad (1)$$

where s is a monotonic function of positions (for holonomic virtual constraints), or positions and velocities (for nonholonomic virtual constraints), and is usually scaled between 0 and 1.

In legged robot applications, s is normally reset every step, and continuity is preserved by imposing equality conditions on h and $\partial h / \partial q$ at $s = 0$ and $s = 1$. This is a convenient choice for legged robots, especially considering there are sensors on both legs for computing the phase variable. For a prosthetic leg application, in order to avoid attaching sensors on the sound leg of the subject, it is desirable to use only onboard sensors from the prosthesis. This is equivalent to resetting the phase variable at the end of each stride, rather than each step. In this case, (1) represents the desired, periodic trajectories for the entire stride.

Due to their dependence on velocities or integrals, nonholonomic virtual constraints are sensitive to changes in speed and are thus not suitable for a controller that is intended to work in a wide range of non-steady activities. A good example is the integral-based unified controller presented in [9], which worked well in normal-speed steady-state walking, but was unreliable for slow speeds and was unable to perform non-rhythmic motions. Therefore, we establish our volitional control scheme on a holonomic phase variable in order to make it speed-independent.

In [19], [20], Villarreal et al. used a perturbation experimental setup to examine and compare various combinations of thigh angle, its derivative, and its integral as invariant parameterizations of human walking gaits. Although the best parameterization found in this study was nonholonomic, the global thigh angle was a close second choice. Motivated by this result, and since the holonomicity of the thigh angle makes it an ideal selection for a volitional controller, we use this variable as the basis for our volitional controller. In what follows we show how this angle is used to construct our phase variable.

B. Constructing the Volitional Phase Variable

As mentioned before, we aim to use thigh angle q_h (Fig. 1(b)), for defining our holonomic phase variable. In what follows, we will show how this variable can be used for this purpose and what other measurements are necessary.

Fig. 1(a) depicts the thigh, knee, and ankle angle trajectories during one stride of a normal able-bodied walking gait [1]. Note that the thigh angle is not a monotonic signal throughout the stride. As a result, each value of q_h corresponds to at least two points in the cycle (one in the descending part of q_h and one in the ascending part), making the determination of a unique s based solely on q_h impossible. To avoid this problem, and also to keep the benefits of a holonomic system, we propose to use a set of *piecewise holonomic* virtual constraints. The idea is to divide the gait cycle into different sections, where each section corresponds to a monotonic (either ascending or descending) thigh angle trajectory.

From Fig. 1(a), the thigh angle trajectory during a stride can roughly be divided into two monotonic sections (neglecting the small retraction section at the end); it is descending after heel strike ($t/T = 0$) and through the stance phase until the trajectory reaches its minimum at $t/T = 0.53$, and then becomes ascending. Note that the swing phase starts a little later, at $t/T = 0.63$. An obvious way to transition between these two states is using the sign change of the thigh angle's rate, \dot{q}_h . In practice this proves to be a very sensitive signal, because velocities can change rapidly, which results in large discontinuities in the virtual constraints and in undesirable transitions. For this reason and since these two monotonic sections approximately correspond to stance and swing phases, in [14] a foot contact sensor was used for transition between these two states. The first problem with this approach is that the minimum thigh angle does not exactly correspond to the foot takeoff ($t/T = 0.53$ versus $t/T = 0.63$) and thus part of pushoff will be performed when the leg is already in swing. Moreover, this approach assumes that the thigh angle exactly follows the reference trajectory. If the minimum thigh angle is larger than the reference trajectory's minimum (shorter step), there will be a jump in the virtual constraints. Conversely, if the minimum thigh angle is less than the reference (longer step), the virtual constraint will saturate, which leaves pushoff half-completed. These undesirable features can be seen in the results of [14].

To resolve these problems, we propose to have two supplementary states (in addition to stance and swing) to represent pushoff. The result is depicted in Fig. 1(c) in the form of an FSM with four states, where S1 and S2 pertain to the descending part of the thigh trajectory, and S3 and S4 correspond to the ascending part. Note that S1, S2, and S3 are all parts of the stance phase, and thus for all of these states $FC = 1$ (FC represents foot contact as a binary signal). For this reason, we use other variables to define these transition conditions. Namely, transition from S1 (stance) to S2 (pushoff onset) occurs at a specific thigh angle ($q_h = q_{po}$), and transition from S2 to S3 (pre-swing) occurs when $\dot{q}_h = 0$. The tunable constant q_{po} represents the thigh angle at the start of pushoff and its default value is obtained from the thigh angle at the maximum ankle angle in the reference trajectory (Fig. 1(a), from which $q_{po} = -8.4^\circ$). As previously mentioned, a transition based on velocity is accompanied with the risk of sensitivity and sudden jumps in virtual constraints. Although these jumps would be small due to the small range of thigh angles represented by S2 and S3, we propose a two-step approach to completely eliminate such discontinuities. In the first step, the transitions from S1 to S2 and from S2 to S3 are designed to be unidirectional, resulting in only one possible jump from S2 to S3. To eliminate this single jump, in the second step we reset the associated parameters based on the information from the sensors. This will be explained in the definition of s in what follows.

For S1 and S2, the phase variable can be computed from a shift and scale of the thigh angle:

$$s = \frac{q_h^0 - q_h}{q_h^0 - q_h^{min}} \cdot c, \quad (2)$$

where q_h^0 and q_h^{min} are constants whose default values are touchdown value and the minimum of the reference thigh angle trajectory, respectively. These two parameters can be tuned if the subject prefers a different step length. The constant c is also tunable and is related to the ratio of the stance phase to the whole cycle. The default value of c is the normalized time at which q_h reaches its minimum, which is 0.53 in Fig. 1(a).

Since the transition from S2 to S3 is based on the change of sign of \dot{q}_h , S3 pertains to the ascending part of the thigh angle. To form a continuous phase variable and to avoid jumps at each transition from S2 to S3, we record the values for s and q_h and name them s_m and $q_{h,m}$ respectively. The phase variable in preswing (S3) and swing (S4) phases is then computed from

$$s = 1 + \frac{1 - s_m}{q_h^0 - q_{h,m}} \cdot (q_h - q_h^0) \quad (3)$$

Note that $s = s_m$ at $q_h = q_{h,m}$ and $s = 1$ at $q_h = q_h^0$. For both (2) and (3), the phase variable is saturated between 0 and 1.

An additional factor to consider for the preswing phase is the tendency of the leg to oscillate as the load is removed from it. This is eliminated by imposing a unidirectional filter on the phase variable in S3. That is, in the discrete time instance k :

$$s(k) \geq s(k-1), \quad \text{when } S = S3, \quad (4)$$

where S is the current state. Note that this condition is not required for S2, as it transitions to S3 at the first instance when \dot{q}_h (and hence \dot{s}) crosses zero.

The FSM of Fig. 1(c) together with the phase variable definition in (2) and (3) constitute a control paradigm based on a forward walking scheme. However, a volitional controller needs to also manage situations in which the motion is interrupted or even reversed. Due to the holonomic nature of the designed phase variable, it is invariant to the direction of motion. Therefore, the problem can only arise during transitions. The most critical situation happens when the leg is in swing and it touches the ground behind the body (backward walking). According to Fig. 1(c) the state transitions to S1 and then immediately to S2 (and perhaps S3), which leads to pushoff and does not allow the subject to put weight on the leg. In order to avoid this, we added another state, S5, to the FSM (Fig. 2). This new state keeps the leg in

stance phase when walking backward, and it transitions to pushoff only if the subject resumes moving forward. With this new state, we define the transitions for our volitional controller as follows:

- 1) *Transition from S1 or S5 to S4:* The primary condition for transition between stance and swing is foot contact. However, in conditions such as standing still, if the leg is unloaded for a moment (i.e., shifting weight to the sound leg), a transition to swing can result in a sudden and undesirable flexion of the knee. To avoid this, we require that the transition to swing happens either after pushoff (i.e., through S2 and S3), or directly from S1 or S5 to S4 at maximum thigh angle ($s = 0$). Obviously, for transition from S5 to pushoff, the state first needs to go to S1, as discussed next.
- 2) *Transition from S5 to S1:* This transition happens when the subject steps backward and then decides to move forward. The transition condition is given by $q_h < q_h^{51}$, where q_h^{51} is a tunable constant. Note that $q_h^{51} < q_h^{21}$ in order to avoid direct transition to pushoff.
- 3) *Transition from S4 to S1 or S5:* Since stance is a more reliable state for the subjects (they can put their weight on the leg), the condition for transition from S4 to S1 or S5 is less strict compared to S1 and S5 to S4. When foot contact happens ($FC = 1$), the transition will be to S1 if $q_h \geq q_h^{41}$, otherwise it will be to S5, where q_h^{41} is a tunable constant. Setting q_h^{41} to zero is equivalent to transition from S4 to S1 for a forward step or to S5 for a backward step.

Fig. 2 summarizes the states and the corresponding transitions.

Normative joint trajectories (normal speed on level ground [1]) for the proposed FSM are parameterized as functions of the phase variable using Fourier transform representations as in [9], which serves as the reference for a PD tracking controller. Thereby, noting that the position error for joint i is $e_i = h(s) - q_i$, the commanded motor torque is obtained from

$$\tau_i = K_{p,i}e_i + K_{d,i}\dot{e}_i \quad (5)$$

where $K_{p,i} > 0$ and $K_{d,i} > 0$ are PD gains for joint i .

III. Experiments

A. Hardware Setup

The powered knee-ankle leg used for our experiments is shown in Fig. 3. Each joint is equipped with a Maxon EC-4pole 30, 200 Watt, three-phase brushless DC motor driving the joints through a timing belt and Nook 2-inm lead ball screw. Due to greater torques in the ankle joint, the timing belt ratio for the ankle is twice that for the knee.

The joints and motors are equipped with optical encoders (Maxon 2RMHF for motors and US Digital, EC35 for joints). An IMU sensor (LORD MicroStrain, 3DMGX4-25) is used to

measure the global thigh angle, as shown in Fig. 3. Foot contact condition is determined using a force sensitive resistor sensor (FSR - FlexiForce A401, Tekscan Inc.) located inside the pyramid adapter of the prosthetic foot.

The computation and control is performed offboard via a tethered connection to a dSPACE DS1007 system. The commanded torques from the computer are sent to an Elmo Gold Twitter R80/80 driver, which controls the motors. See [9] for further details on the design of the prosthetic leg.

B. Experimental Protocol

The experiments were conducted with a male left-side transfemoral amputee subject (32 years old, 1.75 m tall, and 76 kg). The experimental protocol was reviewed and approved by the Institutional Review Board (IRB) at the University of Texas at Dallas. The powered prosthesis was attached to the amputee's in-use custom-made socket by a certified prosthetist (Fig. 3). The subject familiarized himself with the powered leg by walking back and forth between a set of handrails (approximately 5.2 m long). This took about 10 minutes.

Once ready, the subject was asked to walk normally on the walkway between the handrails and to stop at the end of the walkway. This experiment was intended to test the ability of the controller for starting from rest, walking forward, and stopping at a specified position.

Subsequently, to examine the invariance of the controller to the direction of motion, we asked the subject to walk backward on the walkway, as well as to perform a combination of forward and backward transitions, which included sudden stops and rapid reversals of the walking direction.

Next, we tested the ability of the subject to step over an obstacle, specifically an 85-mm high wooden block. After this experiment, the subject was asked to kick a soccer ball to demonstrate the fast extension of the powered knee following a quick forward motion of the hip in an activity other than walking. This test concluded the overground experiments.

To test the controller for rhythmic tasks, the subject was asked to step on a treadmill and walk. The treadmill tests were conducted at three different speeds: slow (1.5 mph) for 60 seconds, normal (2.2 mph) for 60 seconds, and fast (3.5 mph) for 30 seconds. The normal speed was selected based on a natural, comfortable gait for the amputee subject, and the fast speed was selected based on the maximum speed that the subject could walk for the duration of 30 seconds.

For all of these activities, the control parameters introduced in Section II-B remained the same (based on previous tuning with an able-bodied subject).

C. Results

A supplemental video of the experiments is available for download. Fig. 4 displays the phase variable and joint angles through an overground forward walking trial. The subject starts from rest (almost vertical leg), walks across the walkway, and stops at the end. The change

of the minimum ankle angle across strides is particularly interesting, as it represents the extent of pushoff. As the subject starts from rest and increases his walking speed, the ankle plantarflexion also increases (i.e., larger pushoff) until the last stride where the subject decreases his speed and pushoff becomes smaller correspondingly.

The results for a backward walking trial are depicted in Fig. 5. The holonomic nature of the controller enables the subject to comfortably reverse his direction of motion and still maintain a smooth gait. Note that the phase variable has a reverse trajectory compared to Fig. 4.

Fig. 6 shows the thigh and knee angles as the subject kicks a soccer ball. Note that the ball is kicked before maximum hip flexion (and hence maximum knee extension), but due to inertias, the leg continues moving forward. After reaching maximum flexion, the thigh retracts and the knee flexes for ground clearance. Finally, the thigh slightly extends forward, causing the knee to extend and the leg to rest on the ground. This shows the benefit of designing knee and ankle controllers based on following the motion of the thigh, which allows the subject to manage all of these maneuvers without difficulty.

Figs. 7(a) to 7(c) depict the results for treadmill tests with slow, normal, and fast speeds. Note that since q_h^0 and q_h^{min} were not changed, the minimum thigh angle is reached later than the reference trajectory during slow walking (Fig. 7(a)). In other words, the ratio of stance to swing duration increases in order to provide extra time to achieve the minimum thigh angle while the foot is constrained to follow the treadmill speed. As the treadmill speed increases, the minimum thigh angle shifts to the left (Figs. 7(b) and 7(c)) and the stance to swing duration ratio decreases. Furthermore, the amplitude of the minimum thigh angle is consistently larger than the reference (about -17° for all three speeds as opposed to -11° for the reference trajectory). This means that the ankle pushoff is not fast enough to quickly reverse the direction of motion of the thigh and prepare it for the swing phase [21]. These observations will be discussed in detail in the next section.

IV. Discussion

A. Advantages of the Method

As the supplemental video presents, the proposed controller enables the subject to accomplish a variety of volitional (walking forward and backward, instantaneous start and stops, walking over obstacles, shooting a soccer ball), and periodic (walking on a treadmill with different speeds) tasks. Although the designed virtual constraints were based on a periodic task (normal-speed walking kinematics), the holonomic nature of the controller helps the subject perform non-rhythmic tasks as well. Unlike previous controllers that used thigh angle to parameterize the gait [9], [14], the proposed controller is not limited to only one type of motion (periodic or non-periodic).

The speed-invariance of the controller and its improved pushoff management also allowed for greater walking speeds compared to [9]. The amputee subject was able to walk at 3.5 mph for a duration of 30 seconds. In a preliminary set of experiments, able-bodied subjects wearing the prosthesis using a bypass were able to reach 4 mph with the controller

developed in this work. The limitation for high speeds primarily originates from the torque saturation of the motors and not from the controller. The inadequate ankle torque during stance and the limited speed of the knee during swing require the users to compensate using torque from their hips, which quickly leads to fatigue at fast speeds.

B. Limitations

The use of a purely holonomic set of virtual constraints also has a limitation. There is a relatively flat section in the middle part of the phase variable plots (normalized time of about 0.5–0.6) in Figs. 7(a) to 7(c), meaning that the rate of the phase variable is almost zero. To investigate the reason for this phenomenon, note that:

$$\dot{s} = \frac{ds}{dq_h} \dot{q}_h \quad (6)$$

which means for $\dot{q}_h = 0$, we will have $\dot{s} = 0$. This condition occurs during pushoff (transition from S2 to S3). As a result of $\dot{s} = 0$, the knee and ankle rates also tend to vanish, and pushoff becomes slower. This contributes to the thigh continuing backward, before the ankle plantarflexion increases enough to stop the backward motion and drives the thigh forward. This is intrinsic to the holonomic virtual constraints and can be regarded as a trade-off.

Another observation from the treadmill test was the stance to swing duration ratio. Note that the leg's joint kinematics and especially the maximum and minimum of thigh angle change as walking speed varies. For the present study, we kept the kinematics (virtual constraints) unchanged, in order to demonstrate the ability of the controller to work in different situations with minimal tuning. As a result, for low speeds the stance to swing duration ratio was greater than expected. However, walking speed can be detected using fairly straightforward methods (see [3], for example), and kinematics can be changed accordingly. A similar idea can incorporate the necessary kinematic differences between forward and backward trajectories. Note that adding these additional virtual constraints is merely a kinematic modification, whereas the dynamic joint attributes (i.e. joint impedances) remain unchanged. This helped the phase-based controller that was proposed and tested in our previous work be subject independent [9], and we hypothesize this will be the case for the present controller as well.

V. Conclusion

A controller for volitional control of a range of periodic and non-periodic tasks was designed for powered knee-ankle prostheses and validated through experiments with an above-knee amputee subject. The controller uses a phase variable defined as a piecewise holonomic function of the thigh angle with transitions based on a finite state machine.

Although the controller facilitates a wider range of tasks than walking, it does not encapsulate other tasks such as stair ascent and descent. However, the structure provided is flexible for incorporating new sets of kinematics in a task-recognition [22]–[24] or unifying [25] framework.

In the next steps of this work, we will compare the performance of the controller with passive prostheses across a range of tasks. Also, as shown theoretically and observed in the experiments, the holonomic nature of the controller results in a “pause” during pushoff. An interesting extension of the controller would be to include a correction for this interruption in pushoff for a faster and smoother transition to the swing phase. Furthermore, we plan to test the controller on our newly designed leg [26], which provides greater torques as well as backdrivability. These investigations will provide a better understanding of the controller’s abilities, benefits, and potential improvements.

Supplementary Material

Refer to Web version on PubMed Central for supplementary material.

Acknowledgment

The authors would like to thank Christopher Nesler and Emma Reznick from University of Texas at Dallas and Leslie Gray from University of Texas Southwestern for their help in conducting the experiments.

This work was supported by the National Institute of Child Health & Human Development of the NIH under Award Number DP2HD080349. This work was also supported by NSF Award 1734600. The content is solely the responsibility of the authors and does not necessarily represent the official views of the NIH or the NSF. R. D. Gregg holds a Career Award at the Scientific Interface from the Burroughs Welcome Fund.

References

- [1]. Winter DA, Biomechanics and Motor Control of Human Movement. John Wiley & Sons, 2005.
- [2]. Sup F, Bohara A, and Goldfarb M, “Design and control of a powered transfemoral prosthesis,” *Int. J. Robot. Res.*, vol. 27, no. 2, pp. 263–273, 2008.
- [3]. Lenzi T, Hargrove L, and Sensinger J, “Speed-Adaptation Mechanism: Robotic Prostheses Can Actively Regulate Joint Torque,” *IEEE Robot. Autom. Mag.*, vol. 21, no. 4, pp. 94–107, 12 2014.
- [4]. Simon AM, Ingraham KA, Fey NP, Finucane SB, Lipschutz RD, Young AJ, and Hargrove LJ, “Configuring a powered knee and ankle prosthesis for transfemoral amputees within five specific ambulation modes,” *PLoS One*, vol. 9, no. 6, pp. 1–10, 6 2014.
- [5]. Lawson BE and Goldfarb M, “Impedance and Admittance-Based Coordination Control Strategies for Robotic Lower Limb Prostheses,” *ASME Dynamic Systems and Control Magazine*, vol. 136, no. 9, pp. S12–S17, 2014.
- [6]. Lawson BE, Ruhe B, Shultz A, and Goldfarb M, “A Powered Prosthetic Intervention for Bilateral Transfemoral Amputees,” *IEEE Trans. Biomed. Eng.*, vol. 62, no. 4, pp. 1042–1050, Apr. 2015. [PubMed: 25014950]
- [7]. Gregg RD, Lenzi T, Hargrove LJ, and Sensinger JW, “Virtual constraint control of a powered prosthetic leg: From simulation to experiments with transfemoral amputees,” *IEEE Trans. Robot.*, vol. 30, no. 6, pp. 1455–1471, Dec. 2014. [PubMed: 25558185]
- [8]. Villarreal DJ and Gregg RD, “A survey of phase variable candidates of human locomotion,” in *Proc. IEEE Int. Conf. Eng. Med. Biol. Soc.*, Aug. 2014, pp. 4017–4021.
- [9]. Quintero D, Villarreal D, Lambert D, Kapp S, and Gregg R, “Continuous-Phase Control of a Powered Knee-Ankle Prosthesis: Amputee Experiments Across Speeds and Inclines,” *IEEE Trans. Robot.*, vol. 34, no. 3, pp. 686–701, 2018. [PubMed: 30008623]
- [10]. Ha KH, Varol HA, and Goldfarb M, “Volitional control of a prosthetic knee using surface electromyography,” *IEEE Trans. Biomed. Eng.*, vol. 58, no. 1, pp. 144–151, Jan. 2011. [PubMed: 20805047]
- [11]. Hargrove LJ, Simon AM, Lipschutz RD, Finucane SB, and Kuiken TA, “Real-Time Myoelectric Control of Knee and Ankle Motions for Transfemoral Amputees,” *JAMA*, vol. 305, no. 15, p. 1542, Apr. 2011. [PubMed: 21505133]

- [12]. Hoover CD, Fulk GD, and Fite KB, "Stair Ascent With a Powered Transfemoral Prosthesis Under Direct Myoelectric Control," *IEEE/ASME Trans. Mechatron*, vol. 18, no. 3, pp. 1191–1200, Jun. 2013.
- [13]. Hargrove LJ, Simon AM, Young AJ, Lipschutz RD, Finucane SB, Smith DG, and Kuiken TA, "Robotic Leg Control with EMG Decoding in an Amputee with Nerve Transfers," *New Eng. J. Med*, vol. 369, no. 13, pp. 1237–1242, Sep. 2013. [PubMed: 24066744]
- [14]. Villarreal DJ, Quintero D, and Gregg R, "Piecewise and Unified Phase Variables in the Control of a Powered Prosthetic Leg," in *Proc. IEEE Int. Conf. Rehabil. Robot.*, London, UK, 2017, pp. 1425–1430.
- [15]. Westervelt ER, Buche G, and Grizzle JW, "Experimental Validation of a Framework for the Design of Controllers that Induce Stable Walking in Planar Biped," *Int. J. Robot. Res.*, vol. 23, no. 6, pp. 559–582, 6 2004.
- [16]. Westervelt ER, Grizzle JW, Chevallereau C, Choi JH, and Morris B, *Feedback Control of Dynamic Bipedal Robot Locomotion*. CRC Press, 2007.
- [17]. Rezazadeh S and Hurst JW, "Toward step-by-step synthesis of stable gaits for underactuated compliant legged robots," in *Proc. IEEE Int. Conf. Robot. Autom.*, Seattle, USA, May 2015, pp. 4532–4538.
- [18]. Griffin B and Grizzle J, "Nonholonomic virtual constraints and gait optimization for robust walking control," *Int. J. Robot. Res.*, vol. 36, no. 8, pp. 895–922, Jul. 2017.
- [19]. Villarreal DJ and Gregg RD, "Unified phase variables of relative degree two for human locomotion," in *Proc. IEEE Int. Conf. Eng. Med. Biol. Soc.*, Aug. 2016, pp. 6262–6267.
- [20]. Villarreal DJ, Poonawala HA, and Gregg RD, "A Robust Parameterization of Human Gait Patterns Across Phase-Shifting Perturbations," *IEEE Trans. Neural Syst. Rehabil. Eng.*, vol. 25, no. 3, pp. 265–278, 3 2017. [PubMed: 27187967]
- [21]. Lipfert SW, Günther M, Renjewski D, and Seyfarth A, "Impulsive ankle push-off powers leg swing in human walking," *J. Exp. Biol.*, vol. 217, no. 8, pp. 1218–28, Apr. 2014. [PubMed: 24363410]
- [22]. Varol H, Sup F, and Goldfarb M, "Multiclass Real-Time Intent Recognition of a Powered Lower Limb Prosthesis," *IEEE Trans. Biomed. Eng.*, vol. 57, no. 3, pp. 542–551, Mar. 2010. [PubMed: 19846361]
- [23]. Young AJ and Hargrove LJ, "A Classification Method for User-Independent Intent Recognition for Transfemoral Amputees Using Powered Lower Limb Prostheses," *IEEE Trans. Neural Syst. Rehabil. Eng.*, vol. 24, no. 2, pp. 217–225, Feb. 2016. [PubMed: 25794392]
- [24]. Bartlett HL and Goldfarb M, "A Phase Variable Approach for IMU-Based Locomotion Activity Recognition," *IEEE Trans. Biomed. Eng.*, vol. 65, no. 6, pp. 1330–1338, 2018. [PubMed: 28910754]
- [25]. Embry KR, Villarreal DJ, and Gregg RD, "A unified parameterization of human gait across ambulation modes," in *38th Annual Proc. IEEE Int. Conf. Eng. Med. Biol. Soc.*, Aug. 2016, pp. 2179–2183.
- [26]. Elery T, Rezazadeh S, Nesler C, Doan J, Zhu H, and Gregg RD, "Design and Benchtop Validation of a Powered Knee-Ankle Prosthesis with High-Torque, Low-Impedance Actuators," in *Proc. IEEE Int. Conf. Robot. Autom.*, Brisbane, Australia, 2018.

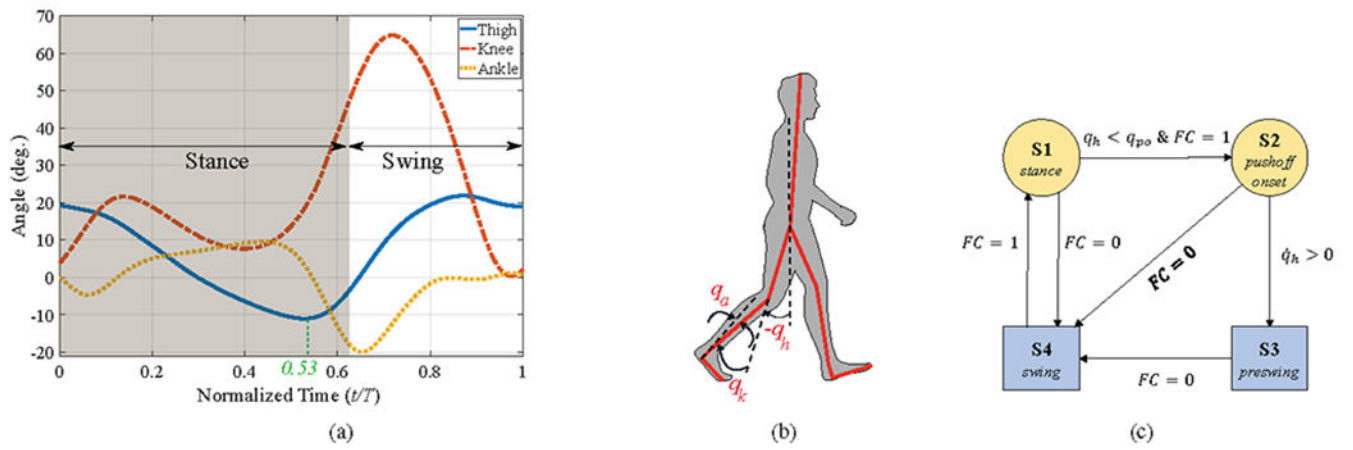


Fig. 1. (a) Joint angle trajectories during one stride of walking with normal speed and stride period $T[1]$. (b) Definition of the joint angles. (c) A preliminary FSM based on forward walking. The phase variable, s , for the yellow circle states is obtained from (2), and for the blue rectangle states from (3).

Author Manuscript

Author Manuscript

Author Manuscript

Author Manuscript

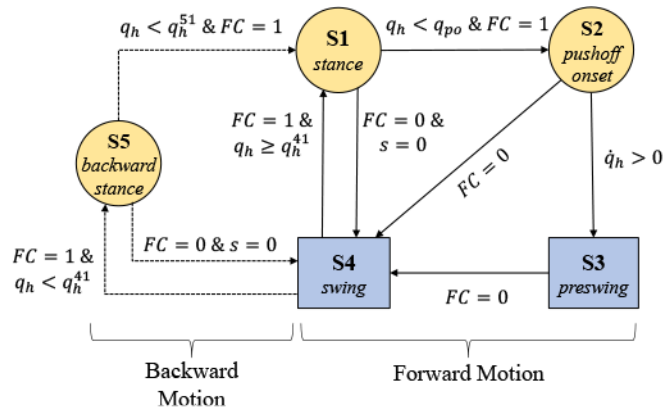


Fig. 2. The complete FSM for computing the phase variable for volitional control of the prosthetic leg. As before, the yellow circles correspond to (2), and the blue rectangles to (3).

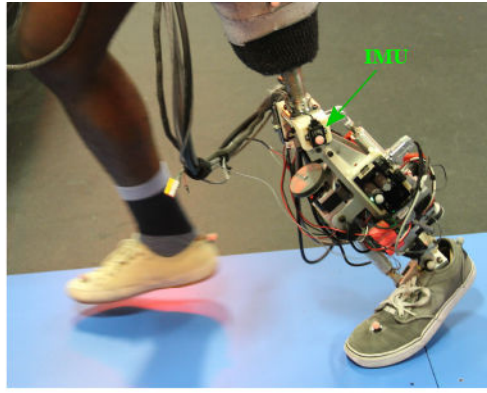


Fig. 3.
The powered knee-ankle prosthetic leg worn by the transfemoral amputee subject.

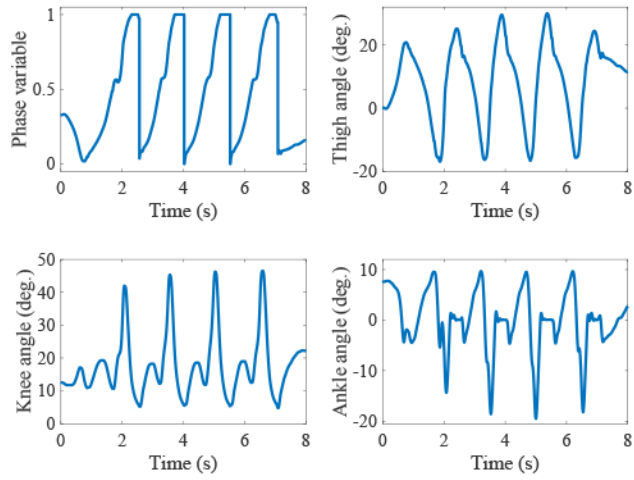


Fig. 4. Phase variable and joint angle plots for a forward walking trial between handrails.

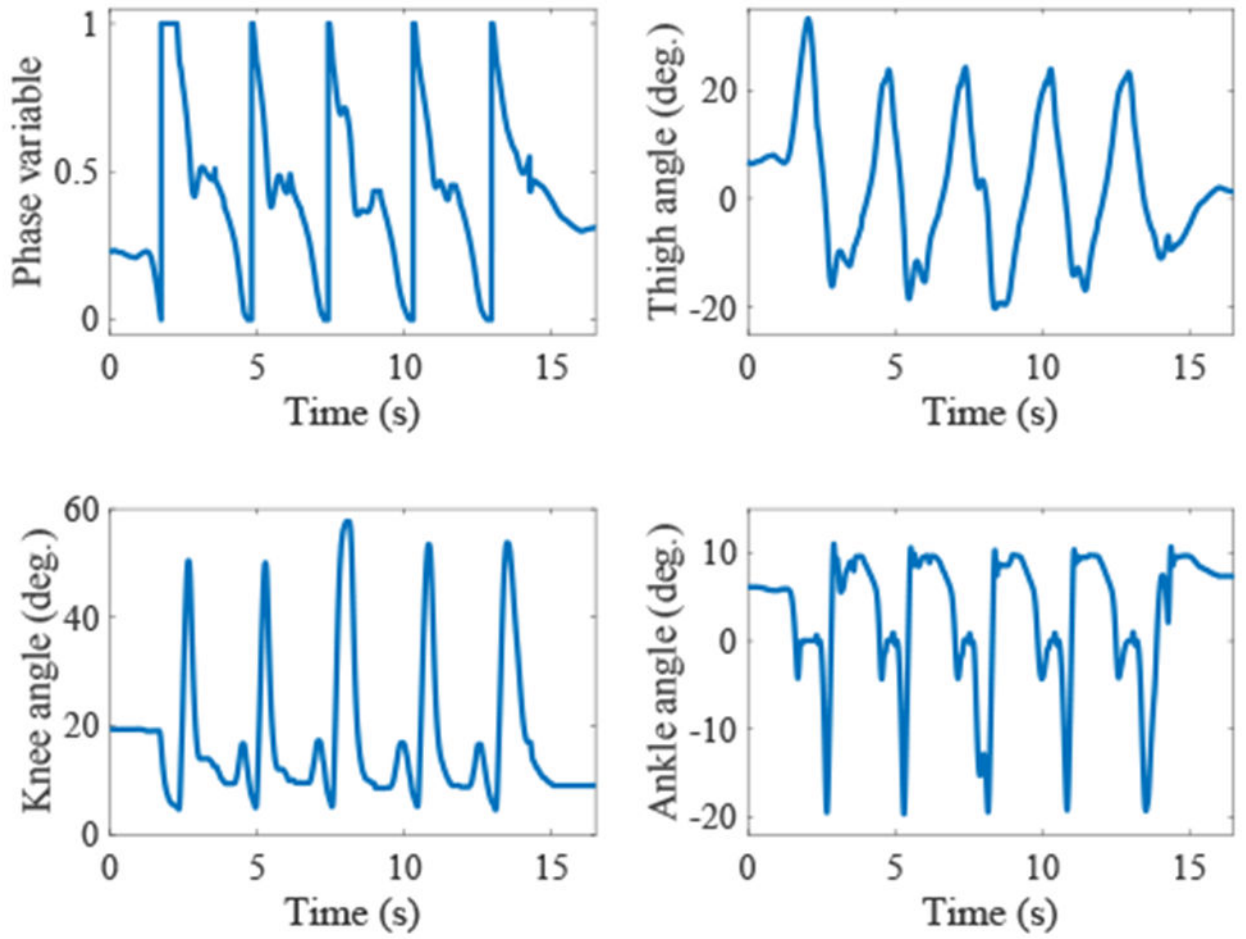


Fig. 5. Phase variable and joint angle plots for a backward walking trial.

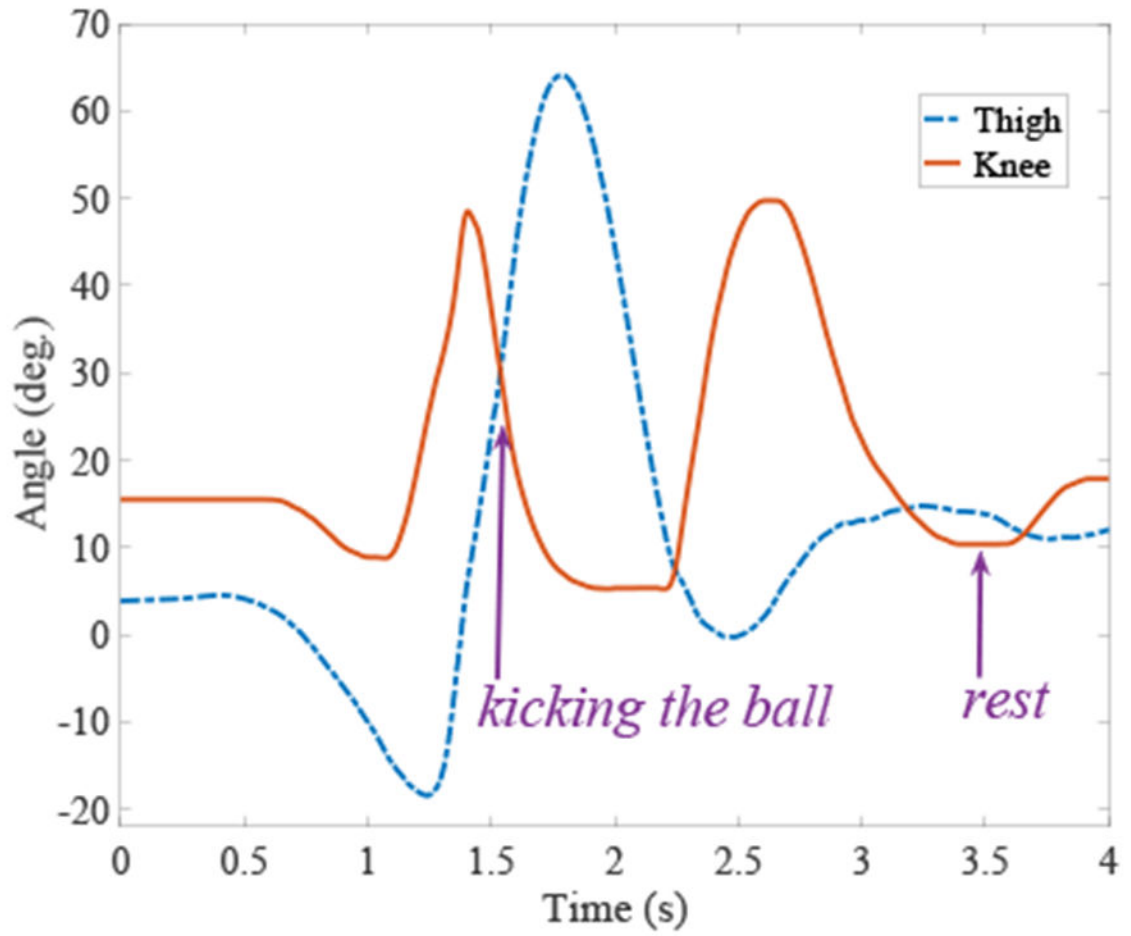


Fig. 6. Thigh and knee angles when shooting a soccer ball with the powered prosthesis. After the shot, the leg retracts and then is placed on the ground (rest).

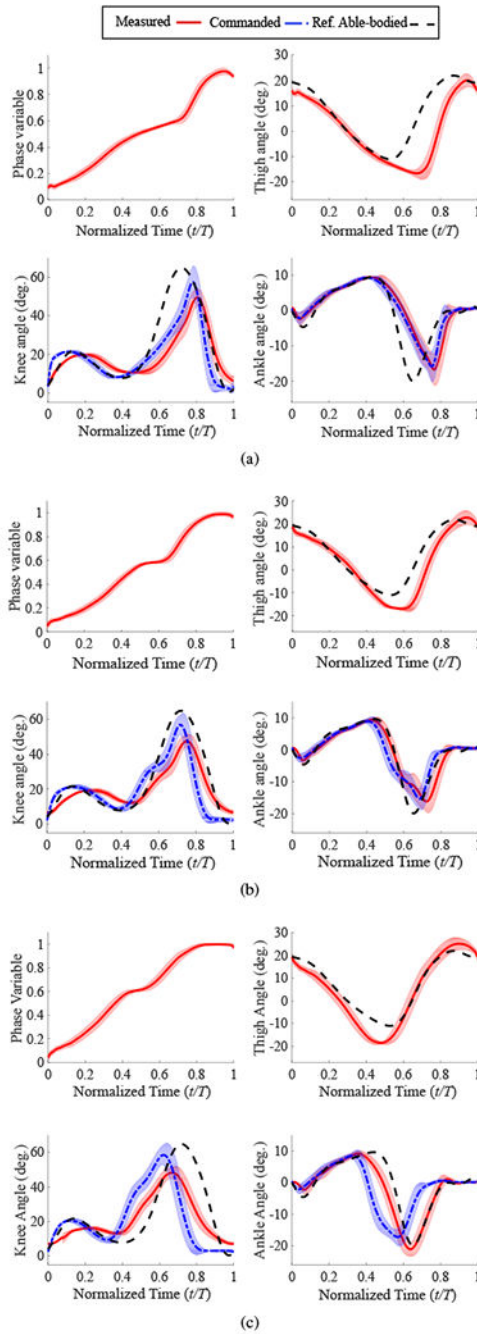


Fig. 7. Mean \pm std for phase variable, and commanded and measured joint angles as a function of normalized time during treadmill test; (a) a 60-second trial with slow speed (1.5 mph) for 21 strides; (b) a 60-second trial with normal speed (2.2 mph) for 32 strides; and (c) a 30-second trial with fast speed (3.5 mph) for 19 strides.